Article

Not peer-reviewed version

Analysis of Spatio-Temporal Patterns of Urban Heat Islands in Kisangani City Using MODIS Imagery: Urban-Rural Gradient, Building Volume Density and Vegetation Effects

Julien Bwazani Balandi , Trésor Mbavumoja Selemani , Jean-Pierre Pitchou Meniko To Hulu , Kouagou Raoul Sambieni , Yannick Useni Sikuzani , Jean-François Bastin , Prisca Tshomba Wola , Jacques Elangilangi Molo , Joël Mobunda Tiko , Bill Mahougnon Agassounon , Jan Bogaert *

Posted Date: 31 December 2024

doi: 10.20944/preprints202412.2623.v1

Keywords: Urban Heat Island; Land Surface Temperature; Building Volume Density; Urbanization Gradient; Kisangani

Article

Analysis of Spatio-Temporal Patterns of Urban Heat Islands in Kisangani City Using MODIS Imagery: Urban-Rural Gradient, Building Volume Density and Vegetation Effects

Julien Bwazani Balandi [1,2], Trésor Mbavumoja Selemani [2], Jean-Pierre Pitchou Meniko To Hulu [3], Kouagou Raoul Sambieni [1,2], Yannick Useni Sikuzani [4], Jean-François Bastin [2], Prisca Tshomba Wola [1], Jacques Elangilangi Molo [1], Joël Mobunda Tiko [1], Bill Mahougnon Agassounon [2,5] and Jan Bogaert [2,*]

[1] Ecole Régionale Postuniversitaire d'Aménagement et de Gestion Intégrés des Forêts et Territoires Tropicaux, Kinshasa P.O. Box 15373, Democratic Republic of the Congo

[2] Unité Biodiversité et Paysage, Gembloux Agro-Bio Tech, Université de Liège, 4000 Liège, Belgium

[3] Institut Facultaire des Sciences Agronomiques de Yangambi, Kisangani P.O. Box 1232, Democratic Republic of the Congo

[4] Unité Ecologie, Restauration Ecologique et Paysage, Faculté des Sciences Agronomiques, Université de Lubumbashi, Lubumbashi P.O. Box 1825, Democratic Republic of the Congo

[5] Laboratoire d'Ecologie, de Botanique et de Biologie végétale (LEB), Université de Parakou, 03 BP125, Benin

* Correspondence: j.bogaert@uliege.be

Abstract: The Urban Heat Island (UHI) effect has emerged in the literature as a major challenge to urban well-being, primarily driven by increasing urbanization. To address this challenge, this study investigates the spatio-temporal pattern of the UHI in the fast-growing city of Kisangani and within its urban-rural gradient from 2000 to 2024. Inferential and descriptive statistics were applied to examine the spatial and temporal patterns of UHI and the relationships between the Land Surface Temperature (LST), building volume density as well as vegetation density expressed by the Normalized Difference Vegetation Index (NDVI). Results showed that the spatial extent of the moderate UHI gradually increased from 16 km² to 38 km², while the high UHI increased from 9 km² to 19 km² between 2000 and 2024. Furthermore, within the urban-rural gradient, significant fluctuations in both LST and UHI are observed, with urban zones exhibiting substantially higher averages than peri-urban and rural zones. LST and UHI variations in the peri-urban areas also differ from those in the rural areas. Moreover, the LST variations are significantly correlated with the building volume density and vegetation density. However, the influence of vegetation density as a predictor of LST gradually decreases while the influence of building volume density increases over time, suggesting the need to implement a synergistic development pathway to manage the interactions between urbanization, landscape change, and ecosystem service provision. This integrated approach may be a key solution to reduce the impact of UHI.

Keywords: Urban Heat Island; Land Surface Temperature; Building Volume Density; Urbanization Gradient; Kisangani

1. Introduction

Increasing urbanization at global, regional, and local scale levels fosters a wide range of environmental challenges, including the urban heat islands (UHI) [1,2]. The urban heat island phenomenon arises from the temperature contrast between rural and urban zones, whereby the daily thermal amplitude of urban zones is decreased as a result of the diurnal absorption of solar energy, which gradually dissipates during the night [3]. Several factors, often summarized into two different but related processes, explain the urban heat island phenomenon. Firstly, and most importantly, the

Preprints.org (www.preprints.org) | NOT PEER-REVIEWED | Posted: 31 December 2024 doi:10.20944/preprints202412.2623.v1

land use and land cover transformations resulting from urbanization, promote increased usage of materials with greater potential for heat absorption and storage, such as asphalt [4]. Furthermore, changes in urban architecture involving building geometry, particularly construction patterns with tall buildings situated closely together in small spaces, contribute to the phenomenon referred to as the "urban canyon"[5,6]. This urban canyon effect influences various local conditions, including wind patterns, light availability, air quality, and temperature, thereby significantly exacerbating the urban heat islands (UHI) effects [7]. Secondly, thermal emissions resulting from human activities, particularly from transport and industrial activities, further amplify surface warming [8].

The UHI effect is typically related to various environmental, social, and economic consequences. This can significantly affect city residents in a variety of interconnected ways. Beyond compromising well-being, raising energy consumption, and deteriorating air quality, the UHI effect can aggravate respiratory health problems. Elevated heat places strain on water supply systems, reducing availability and increasing contamination risks, particularly in areas dependent on vulnerable water sources [9–11]. The UHI effect disrupts cultural and social dynamics by limiting outdoor activities and altering the natural rhythms of urban life. Especially in tropical areas, such as the Kisangani region in the Democratic Republic of Congo (DRC), the UHI effect may significantly impact agriculture, where high temperatures already pose challenges. Indeed, elevated urban heat alters microclimates [7], with the potential to spread parasites and diseases that thrive in warmer conditions, increase irrigation requirements, and accelerate the decomposition of soil organic matter, thereby reducing fertility. The UHI effect has thus attracted considerable attention, particularly in the last decade, due to such challenges.

In this context, Garcia-Herrera et al. [12], conducted an extensive analysis of the 2003 Extreme Heat Wave (EHW 03) and found that France showed the highest mortality increase during this event. Between August 4 and 13, air temperatures were exceptionally unusual, both in their intensity and duration. During the period from August 1 to 20, mortality rates rose by 60% compared to the 1999-2002 average for the same timeframe, resulting in an additional 14,802 deaths. In Shanghai, China, Zhang et al. [13] demonstrated that shifts in land use and land cover (LULC), coupled with population changes, have significantly altered the spatial and temporal dynamics of the UHI, largely driven by the reduction of water bodies and green spaces. In the United Kingdom (UK), Malley et al. [14] examined the effective and resilient mitigation strategies of UHI and guided their future application. Findings highlight that the design elements of buildings, including their shape, orientation, and arrangement, have a crucial role in mitigating UHI effects. In addition, the incorporation of green spaces and the use of highly reflective materials are highly effective in reducing urban heat.

In India, Mandal et al.[15], investigated the growth of the UHI effect within the Kolkata Metropolitan Area (KMA) and its surroundings, revealing that the land surface temperature (LST) has risen significantly in both regions, with the KMA experiencing an increase of 2.5 times greater than that of its neighboring areas. In the tropical regions, Li et al.[16], investigated the effects of urbanization on the intensity of the UHI phenomenon in Kampala, Uganda, and found that the area affected by the UHI increased significantly between 2003 and 2017, while the average daytime UHI temperature decreased. While the UHI effect has reduced in some areas of Uganda, it has increased in others, indicating that urbanization, if managed effectively, does not necessarily lead to worsening environmental conditions [16]. Furthermore, in the region of Accra, Ghana, Wemegah et al.[17], examined the presence and spatial distribution of the UHI effect and its impact on temperature extremes. The findings confirmed the existence of UHI in the area, with a growing spatial extent and intensity. Built-up areas and bare land were identified as the most impacted by UHI warming, which also intensified the frequency and magnitude of extreme heat events in the region.

While the UHI effect has been widely investigated elsewhere, there is no available research on the existence and effects of the urban heat island in the city of Kisangani, DRC, which underwent significant spatial expansion between 1987 and 2021 [18], resulting in a decline in the composition of mature and short forests and a significant change in its spatial configuration [19]. Therefore, this research aims to address a significant limitation in the existing literature by providing empirical evidence on the spatial and temporal pattern of the UHI, especially in the context of rapid urbanization in the city of Kisangani. In addition, statistical analysis of the historical relationship between urban architecture specifically the height and width of buildings and the LST, performed in this study, offers a new perspective on how architectural dimensions affect thermal dynamics, revealing important insights into the impact of urban design on temperature variations over time. Furthermore, the analysis of the spatio-temporal patterns of the UHI across the urbanization gradient, through randomly selected plots, offers a wider and more comprehensive perspective on the variation in the spatial effects of urban heat islands.

We therefore hypothesize that transformations in Kisangani's spatial pattern between 2000 and 2024, resulting from uncontrolled urban expansion [18–20], have led to variations in Land Surface Temperature (LST), reflected in the formation of Urban Heat Island (UHI). Moreover, the extent of these urban heat islands (UHIs) is expected to have expanded significantly highlighting the intensified effect of urbanization on local thermal conditions.

Within the urbanization gradient, we expect significant fluctuations in both the LST and UHI effect, with urban areas exhibiting substantially higher averages than peri-urban and rural areas, due to the increasing landscape artificialization and the high density of anthropogenic activities in 2024. From 2000 to 2024, annual variations of the LST and the UHI effect are anticipated to differ significantly from one year to the next within each urbanization gradient zone, reflecting their dynamic and evolving nature. In addition, for each year from 2000 to 2023, we anticipate significant differences in the UHI annual fluctuations between urban, peri-urban, and rural areas.

Furthermore, Land Surface Temperature (LST) variations are expected to be significantly correlated with (1) Building Volume Density (BVD), a parameter that integrates footprint (width and length) and height of buildings, and (2) vegetation density, expressed as the Normalized Difference Vegetation Index (NDVI). However, as Kisangani's urban architecture evolves, with increasingly dense and taller buildings, the influence of Building Volume Density (BVD) as a predictor of the LST, and consequently of the UHI effect, is predicted to increase over time (2000-2024), while the role of vegetation density as a predictor of Land Surface Temperature is expected to gradually decrease due to the degradation of green infrastructure.

2. Materials and Methods

2.1. Study Area

The area examined comprises the city of Kisangani and its surroundings in north-eastern DRC (Figure 1). Covering an area of 2,947.9 km², the studied region includes six municipalities of the city of Kisangani. Five of these administrative areas are situated on the right bank of the Congo River, while one is located on the left bank (Figure 1). Over 50 years (1956–2005), the region recorded an average annual rainfall of 1,724 mm and a mean annual temperature of 25.3°C [21]. Monthly rainfall consistently surpasses 60 mm year-round [21], classifying Kisangani as an Af climate type under the Köppen classification system [21,22]. Kisangani reported substantial population growth in recent years. According to the National Statistics Institute, the city's population surpassed 2,184,096 in 2021 [18]. The city is characterized by a diverse mix of ethnic groups from different regions of the DRC and neighboring countries. Most residents sustain their livelihoods through agriculture, fishing, and trade [23]. In recent years, the rising demand for housing and social infrastructure in urban centers has driven significant peri-urban expansion between 2010 and 2021 [18].

Preprints.org (www.preprints.org) | NOT PEER-REVIEWED | Posted: 31 December 2024 doi:10.20944/preprints202412.2623.v1

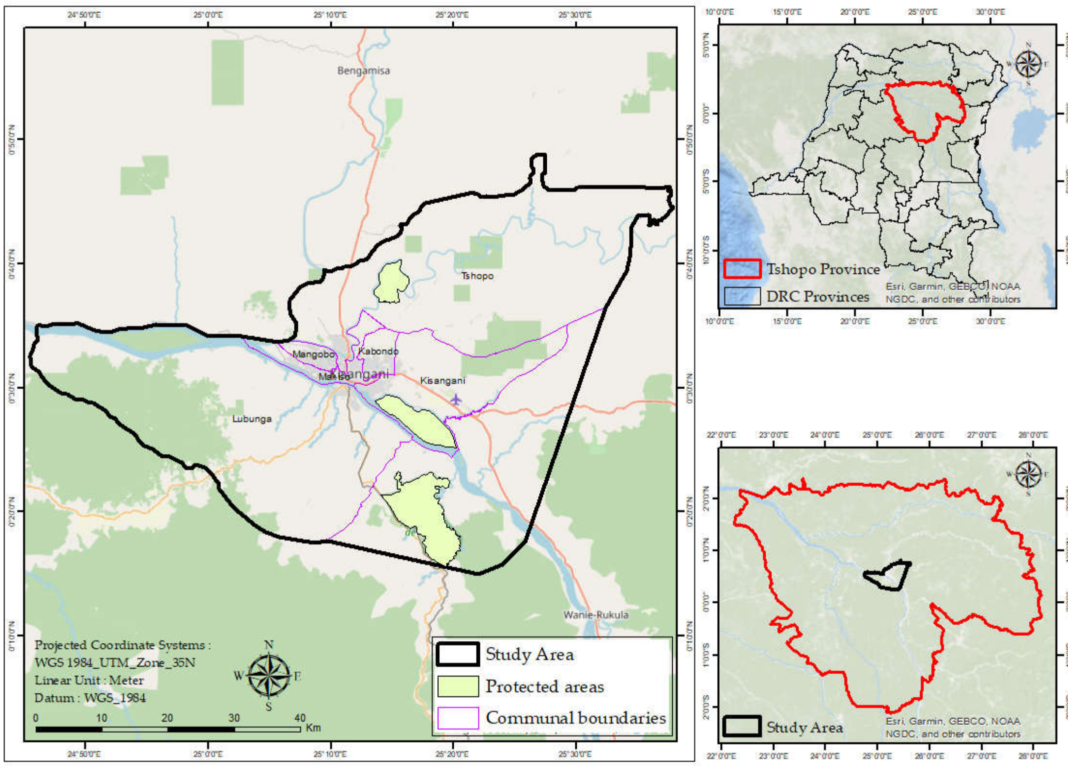

Figure 1. Kisangani and its surrounding area. The city is organized into six municipalities and is surrounded by three protected areas. Its transport infrastructure includes both national and provincial road networks.

2.2. Data Used

Spatio-temporal pattern analysis of urban heat island (UHI) and vegetation density as measured by NDVI, were performed using MODIS satellite data available in Google Earth Engine. Data regarding building volume was obtained from the Global Human Settlement Layer (GHSL) project of the Joint Research Centre (JRC) as updated in 2023 [24]. Furthermore, high-resolution satellite imagery from Google Earth was employed to identify and characterize urban, peri-urban, and rural zones along the urbanization gradient. Table 1 below describes the data used.

Table 1. The collected geospatial data.

Product ID	Layer	Spatial Resolution	Time scale
MOD11A2 V6.1	LST Emissivity	1000m	01.01 – 31.12
MOD13A2	NDVI	1000m	01.01.– 31.12
GHS-BUILT-V	Building Volume	1000m	Annual
Google Earth	GE Images	1m	Annual

2.3. Data-Processing and Derivation of the Land Surface Temperature (LST)

Google Earth Engine (GEE) platform provides access to MODIS Land Surface Temperature (LST) products through the "MOD11A2 V6.1" image collection. Each pixel in MOD11A2 represents the mean value derived from all corresponding MOD11A1 LST pixels recorded over the 8-day interval [25]. The daily MOD11A1 LST product is generated using pixel-level LST data from individual granules, derived under clear-sky conditions through the generalized split-window algorithm. This method adjusts LST values in two thermal infrared bands (31 and 32) to compensate for atmospheric influences. Additionally, it incorporates land-cover-specific emissivity values to refine LST accuracy

Preprints.org (www.preprints.org) | NOT PEER-REVIEWED | Posted: 31 December 2024 doi:10.20944/preprints202412.2623.v1

by addressing variations in surface emissivity [25,26]. Using GEE, the LST images were transformed from Kelvin to Celsius by applying a scale factor of 0.02 and subtracting 273.15 [15–25].

We used the NDVI to quantify variations in vegetation density. NDVI is derived from the visible and near-infrared (NIR) bands of the Advanced Very High-Resolution Radiometer (AVHRR) and MODIS, particularly using the "MODIS/061/MOD13A2" dataset. This collection provides NDVI images at 1 km spatial resolution with a 16-day interval. Generally, positive NDVI values signify vegetated areas, whereas values at or below zero represent bare soil or water bodies [26,27].

The geospatial data on building volume used in this study was obtained through the Global Human Settlement Layer (GHSL) project [24]. This raster dataset depicts the worldwide distribution of building volumes, measured in cubic meters, with a spatial resolution of 1 km. It provides data on the total building volume and the volume associated with grid cells primarily designated for non-residential (NRES) purposes. These estimates are derived from built-up surface and building height data, generated using inputs from Advanced World 3D 30m (AW3D30), Shuttle Radar Topography Mission (SRTM30), Sentinel-2, and Landsat composites [24]. The data cover the period from 1975 to 2030 and are spatio-temporally interpolated at five-year intervals. Data for the intermediate years were derived through a straightforward analysis of annual rate changes. For instance, the data for 2001, 2002, 2003, and 2004 were obtained by applying the annual percentage change calculated between 2000 and 2005.

2.4. Derivation of the Urban Heat Island (UHI)

The mean LST in rural areas was used to indicate the mean LST in the whole study area in order to analyze the UHI effect [13–29]. This analysis was conducted to evaluate temperature fluctuations across urban, peri-urban, and rural zones. Therefore, the UHI effect for each zone can be calculated as :

$$\boldsymbol{UHI} = \Delta T / \, T_s \; = (T_i - T_s)/T_s \tag{1}$$

Where: UHI refers to the urban heat island effect (UHI), measured as the relative LST in the area; ΔT is the difference between the i-th pixel LST (Ti) and the average rural LST (Ts). From the overall comprehension of the spatial and temporal pattern of the UHI, the UHI magnitude can be categorized into five levels [28,29] (Table 2).

Table 2. The UHI level.

UHI (°C)	Level	Description
UHI ≤ 0	Very low	Extreme low-temperature zone, meaning that there is no difference in LST between urban and rural areas.
0<UHI ≤ 0.1	Low	Low-temperature zone, which means that the LST variation between urban and rural areas is minimal.
0.1<UHI ≤ 0.2	Medium	Medium temperature region, meaning that the LST differs moderately between urban and rural areas.
0.2<UHI ≤ 0.3	High	High-temperature zone, meaning large urban/rural LST difference.
0.3<UHI	Very high	Extremely high-temperature zone, meaning very large urban/rural LST difference.

2.5. Spatial Analysis and Delineation of Urban-Rural Gradient Zones

Analysis of Urban Heat Island (UHI) was conducted within the urban-rural gradient of Kisangani city. Spatiotemporal analyses of the UHI effect across the urban-rural gradient are in many cases conducted using either a transect-based approach [30], or a concentric zone method [15]. However, to improve our understanding of the UHI phenomenon across the urban-rural gradient, we used a methodology that captures the spatial complexity inherent in the landscape. To achieve this, a strategic randomized sampling approach was adopted, selecting plots in different directions: north, south, east, and west, as well as north-east, north-west, south-east, and south-west within each defined area of the gradient. This approach not only enriches the data collected, but also accounts for the significant spatial variation that can occur perpendicular to a traditional transect. By capturing and incorporating variation at short distances, this approach avoids potential oversights that a concentric zone methodology might introduce [19].

To delineate the urbanization gradient zones, built-up areas, which represent one of the most precise, consistent, and evolving morphological indicators [18–32], were analyzed annually. For each date, from 2000 to 2024, high-resolution satellite data available on Google Earth were used. Indeed, using a Geographic Information System (GIS), the intensity level of each pixel was highlighted in a range from 0 to 255. Built-up pixels, characterized by impermeable surfaces (roads, roofs, and compacted floors) were assigned intensity values ranging from 80 to 255. Agricultural and grassland pixels were assigned intensity values ranging from 50 to 80 depending on the evolution stage (cultivated land or fallow land). However, forest pixels were characterized by intensity values below 50. Thus, for each year, a plot is classified as urban if more than 50% of its area is covered by built-up pixels. Conversely, a parcel with 50% or fewer built-up pixels is considered peri-urban, as long as the remaining pixels do not exclusively represent forest or agricultural zones. On the other hand, a parcel is considered rural if it consists mainly of vegetation.

A total of 86 plots (Figure 2), each covering a spatial dimension of 1 km², corresponding to the spatial resolution of the MODIS data used, were randomly selected from each zone in the reference year (2024). The random sampling technique was employed to reduce potential bias and improve the applicability of the results on the landscape scale. This method is essential to provide an objective assessment of the variability present in the landscape and to provide a complete view of the impact of urbanization on the UHI phenomenon across the urban-rural gradient. However, it is important to note that spatial features in these observation plots have evolved, reflecting the dynamic properties of urban, peri-urban, and rural zones.

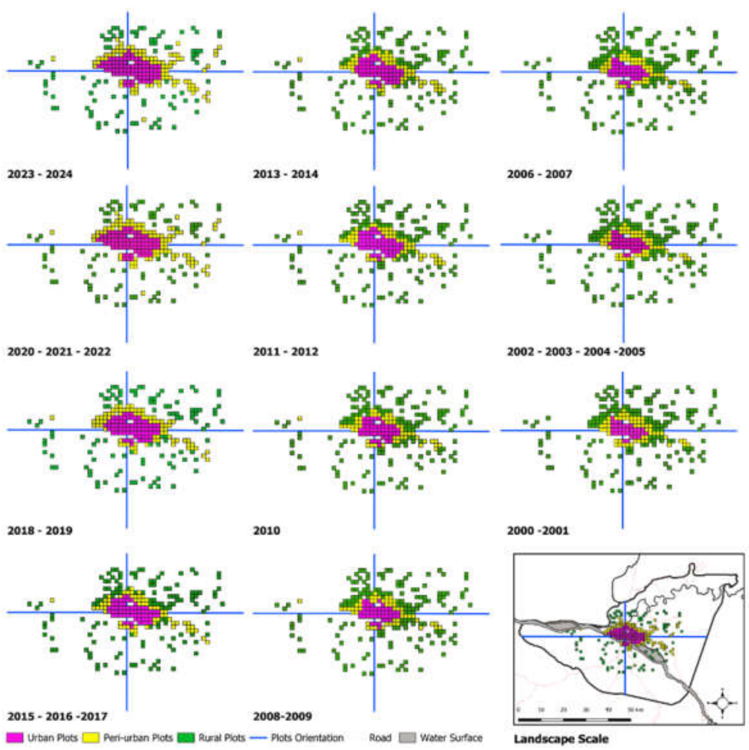

Figure 2. Sample plots along the Urban-Rural Gradient. A series of randomly selected sample plots were analyzed along the urban-rural gradient, encompassing various directional perspectives: north, south, east, west,

Preprints.org (www.preprints.org) | NOT PEER-REVIEWED | Posted: 31 December 2024 doi:10.20944/preprints202412.2623.v1

northeast, northwest, southeast, and southwest. The evolving characteristics of these plots highlight the dynamic and continual shifting of urban, peri-urban, and rural areas.

As samples have satisfied the key assumptions for parametric tests, including data normality and homogeneity of variances, we applied an analysis of Variance (ANOVA) test to assess the spatial variations of the LST and the UHI effect across urban, peri-urban, and rural zones. Additionally, this approach was employed to assess the temporal effects of various years on LST and UHI variations. Furthermore, to assess the impacts of Building Volume Density (BVD) and vegetation density, we conducted linear regression analyses. The historical trends observed in the slope and coefficient of determination from these regressions have enhanced our understanding of the roles of building volume density and vegetation density as predictors of LST.

3. Results

3.1. Spatio-Temporal Patterns of Urban Heat Island (UHI)

The spatial pattern of Urban Heat Islands (UHI) exhibits significant temporal variation. From 2000 to 2009, the landscape of Kisangani was predominantly dominated by areas with UHI values at or below 0°C, lowest UHI values consistently observed along river corridors. In contrast, between 2010 and 2024, areas with UHI values exceeding 0°C expanded considerably, significant annual UHI values, exceeding 0.1 and 0.2°C consistently observed in the city center (Figure 3). Furthermore, the spatial extent of medium UHI gradually expanded from 16 km² to 38 km², while high UHI increased from 9 km² to 19 km². Consequently, the total extent of UHIs greater than 0.1°C reached more than 50 km² in 2024 (Figure 4).

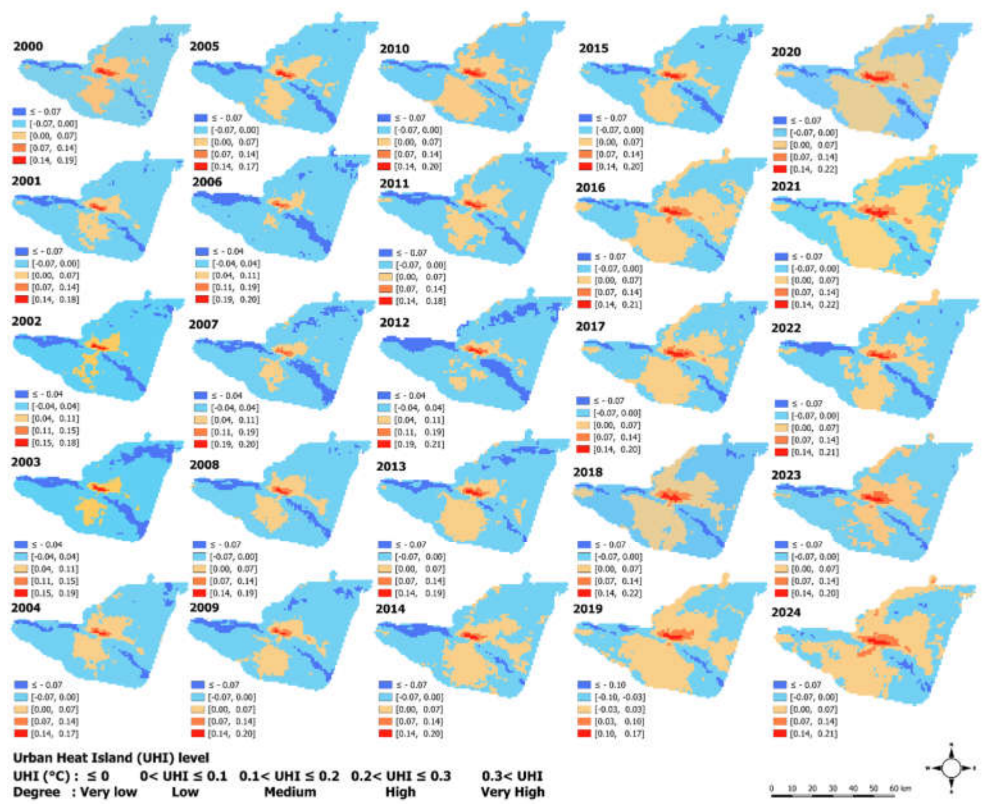

Figure 3. Spatial variations of diurnal Urban Heat Island (UHI). The UHI corresponds to Land Surface Temperature (LST) per pixel relative to the Rural Average Temperature. Data from MODIS sensor (MOD11A2 V6.1) covering the period from 2000 to 2024.

Preprints.org (www.preprints.org) | NOT PEER-REVIEWED | Posted: 31 December 2024 doi:10.20944/preprints202412.2623.v1

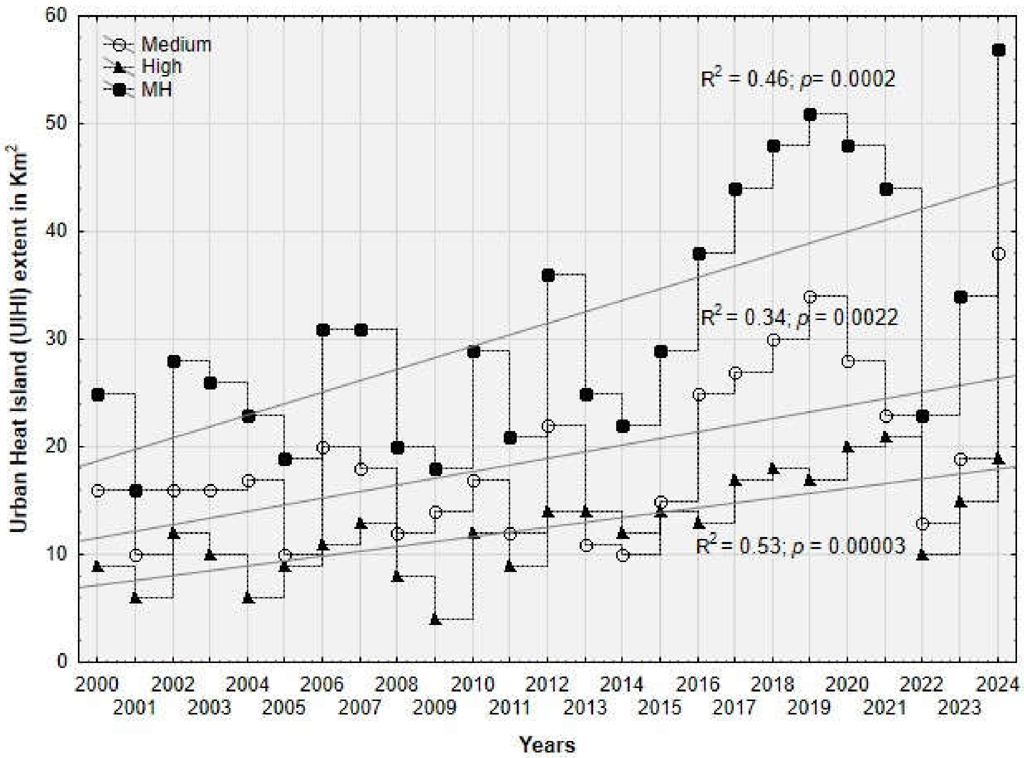

Figure 4. The spatial extent of Urban Heat Islands (UHI) is expressed in square km. Medium (0.1<UHI<0.2); High (0.2<UHI≤0.3); MH expresses the sum of Medium and High UHI extent.

3.2. Variation in LST and UHI Across the Urban-Rural Gradient in 2024

Within the Urban-Rural Gradient, as expected, significant variations in both Land Surface Temperature (LST) and Urban Heat Island effect (UHI) are observed in 2024, with urban zones exhibiting substantially higher averages than peri-urban and rural zones. LST and UHI variations in peri-urban areas also differ significantly from those observed in rural areas. Furthermore, areas with maximum LST around 34°C and maximum UHI values of more than 0.2°C, are observed in urban zones, while peri-urban and rural zones reach maximum LST of 31°C and maximum UHI values of slightly more than 0.1°C.

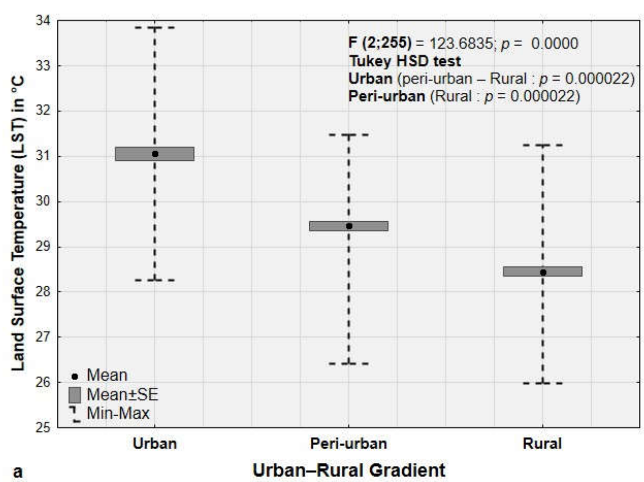

 doi:10.20944/preprints202412.2623.v1

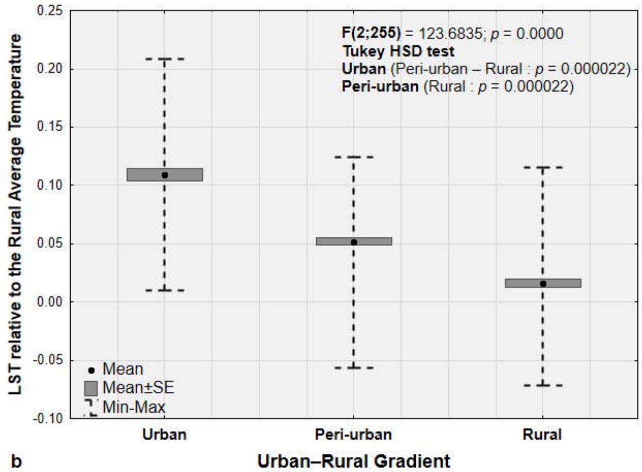

Figure 5. Land Surface Temperature (LST) and Urban Heat Island (UHI) variation in Urban, per-urban, and Rural zones based on the landscape context of the last year studied (2024).

3.3. Historical Variations in LST and UHI Across the Urban-Rural Gradient

Statistical analysis revealed significant historical trends in annual land surface temperature (LST) and urban heat island (UHI) variations within each urbanization gradient zone from 2000 to 2024 ($p < 0.05$). Tukey's post hoc tests identified specific years with significant differences within each gradient, indicating notable temporal shifts.

In urban areas, notable differences in LST were observed between earlier years (e.g., 2000, 2003, and 2006) and more recent years such as 2018, 2019, and 2021. For instance, 2000 significantly differs from 2012, and 2003 differs from 2018, 2019, and 2021. Additionally, 2012 shows significant variations compared to a broader range of years, including 2017, 2018, 2019, 2020, and 2024. UHI variations similarly highlight significant differences between earlier years (e.g., 2000, 2002, and 2003) and recent periods such as 2019 and 2022, with 2022 also differing significantly from 2024.

In peri-urban zones, significant differences in LST (Land Surface Temperature) were observed across multiple time intervals. Early years, such as 2000 and 2001, showed significant differences with later years, including 2002, 2003, 2006, 2007, 2012, 2013, and 2022. For example, 2002 differed significantly from 2010, 2016–2020, and 2024, while 2003 differed from both earlier years like 2004 and later years such as 2016–2020, 2023, and 2024. Similarly, more recent years, such as 2012-2015, showed significant variations compared to 2016-2024, and 2022 differed significantly from 2024. There were also significant temporal differences in the urban heat island (UHI) variations. Early years, such as 2000 and 2002, showed notable differences with years like 2013–2019 and 2022. For example, 2002 differed significantly from a range of years spanning 2005–2022. Later years, such as 2013–2015, exhibited significant differences from 2016–2024, while 2016–2018 differed from 2019 and 2022. Notable contrasts also emerged between more recent years: for instance, 2022 differed significantly from 2024.

Rural areas showed the widest range of differences in LST and UHI variations. LST differences spanned several pairs of years, such as 2000 vs. (2002, 2006, and 2022) and 2006 vs. (2008, 2017 and 2024). More recent years, such as 2016-2020, were consistently different from earlier periods (e.g. 2012-2015) and from later years, such as 2022 and 2024. For example, LST in 2016 differed significantly from 2022, while 2023 differed from 2024. Similarly, UHI variations in rural areas revealed significant differences between earlier years (e.g., 2000 and 2002) and later periods, such as 2019, 2022, and 2023. For instance, UHI in 2006 and 2007 showed significant differences from multiple years, including 2008, 2016, and 2024. Additionally, 2022 and 2023 exhibited consistent contrasts with 2024, indicating persistent changes in rural thermal environments.

Furthermore, as expected, the results of the annual comparison of the urban heat island (UHI) effect from 2000 to 2024 across Kisangani's urbanization gradients reveal significant differences.

 doi:10.20944/preprints202412.2623.v1

Annual UHI variations in urban zones consistently differed from those in peri-urban and rural zones (p <0.05). Moreover, UHI variations in peri-urban zones were significantly distinct from those observed in rural zones throughout the study period. These findings highlight clear and consistent disparities in UHI dynamics across the urban, peri-urban, and rural gradients.

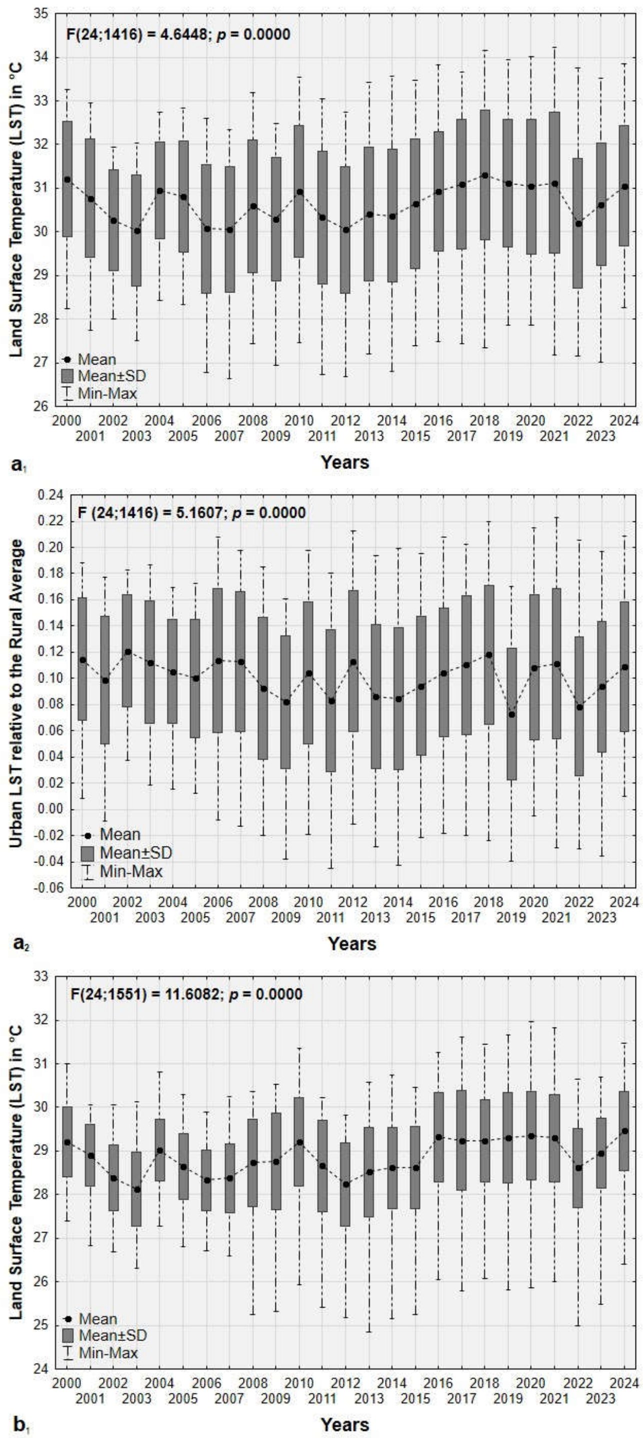

Preprints.org (www.preprints.org) | NOT PEER-REVIEWED | Posted: 31 December 2024 doi:10.20944/preprints202412.2623.v1

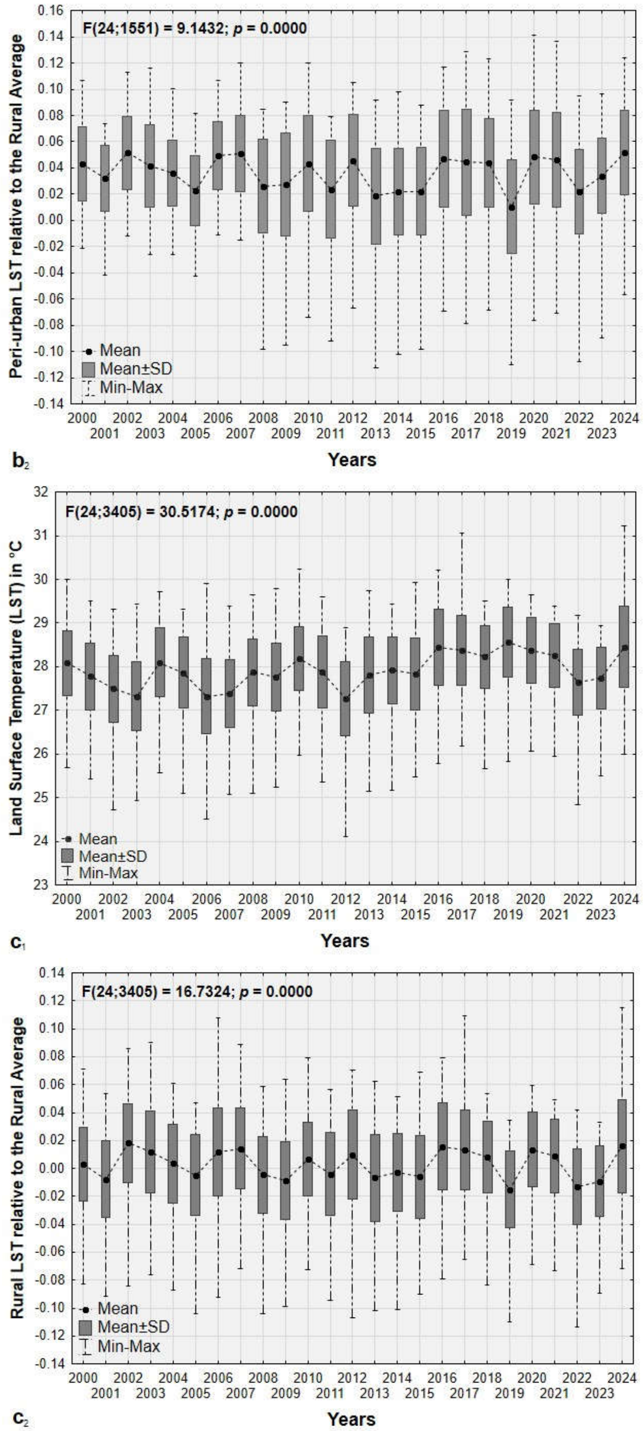

Figure 6. Historical variations in Land Surface Temperature (LST) and Urban Heat Island (UHI) in urban areas (**a**$_1$,**a**$_2$), peri-urban areas (**b**$_1$,**b**$_2$), and rural areas (**c**$_1$,**c**$_2$).

3.4. Building Volume Density (BVD) and Vegetation Effects

As expected, land surface temperature (LST) variations are significantly correlated with the Building Volume Density (BVD) and vegetation density, expressed by the Normalized Difference Vegetation Index (NDVI) (Figure 7a). Moreover, the influence of Building Volume Density (BVD) as a predictor of Land Surface Temperature (LST) increases over time. This trend, evidenced by progressively higher slopes and coefficients of determination values (Figure 7b$_1$c$_1$), highlights the growing role of urban development in shaping thermal patterns. Conversely, the influence of

Preprints.org (www.preprints.org) | NOT PEER-REVIEWED | Posted: 31 December 2024 doi:10.20944/preprints202412.2623.v1

vegetation density as a predictor of Land Surface Temperature (LST), as expected, is gradually decreasing over time. This trend, reflected in progressively lower slope values and coefficients of determination in the regression analyses (Figure 7b2c2), reveals a weakening relationship between vegetation and temperature regulation.

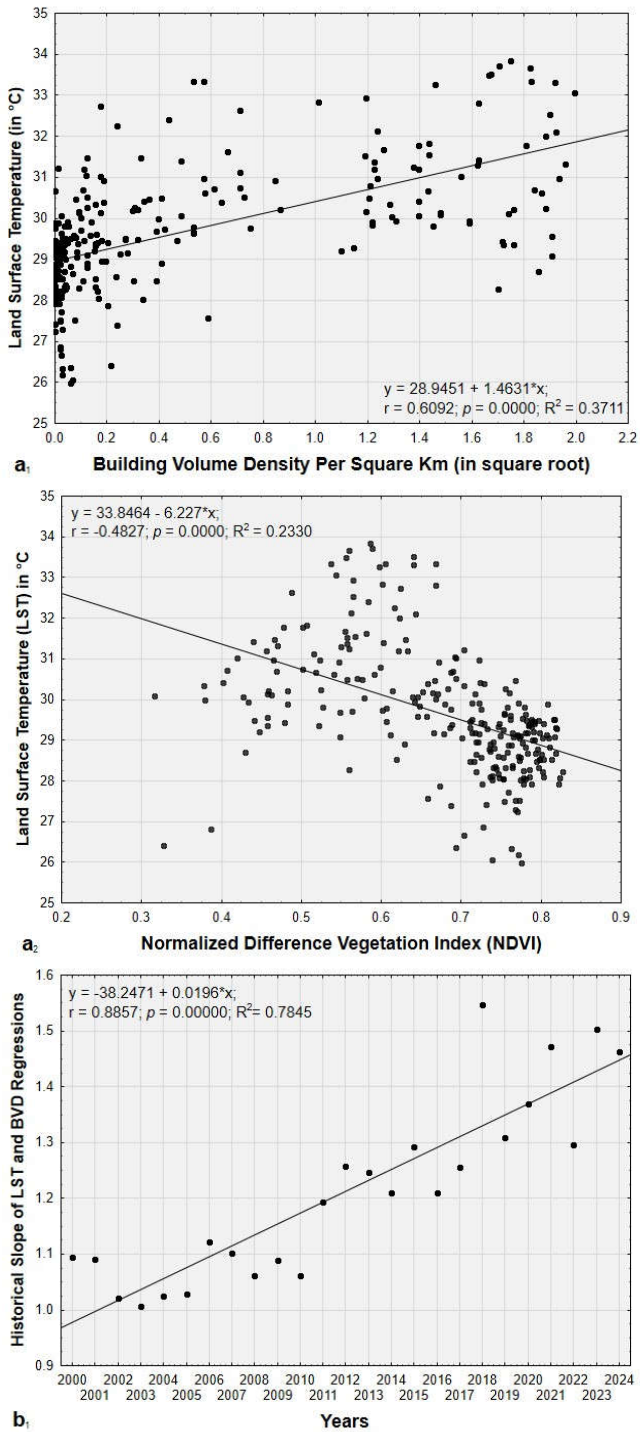

Preprints.org (www.preprints.org) | NOT PEER-REVIEWED | Posted: 31 December 2024 doi:10.20944/preprints202412.2623.v1

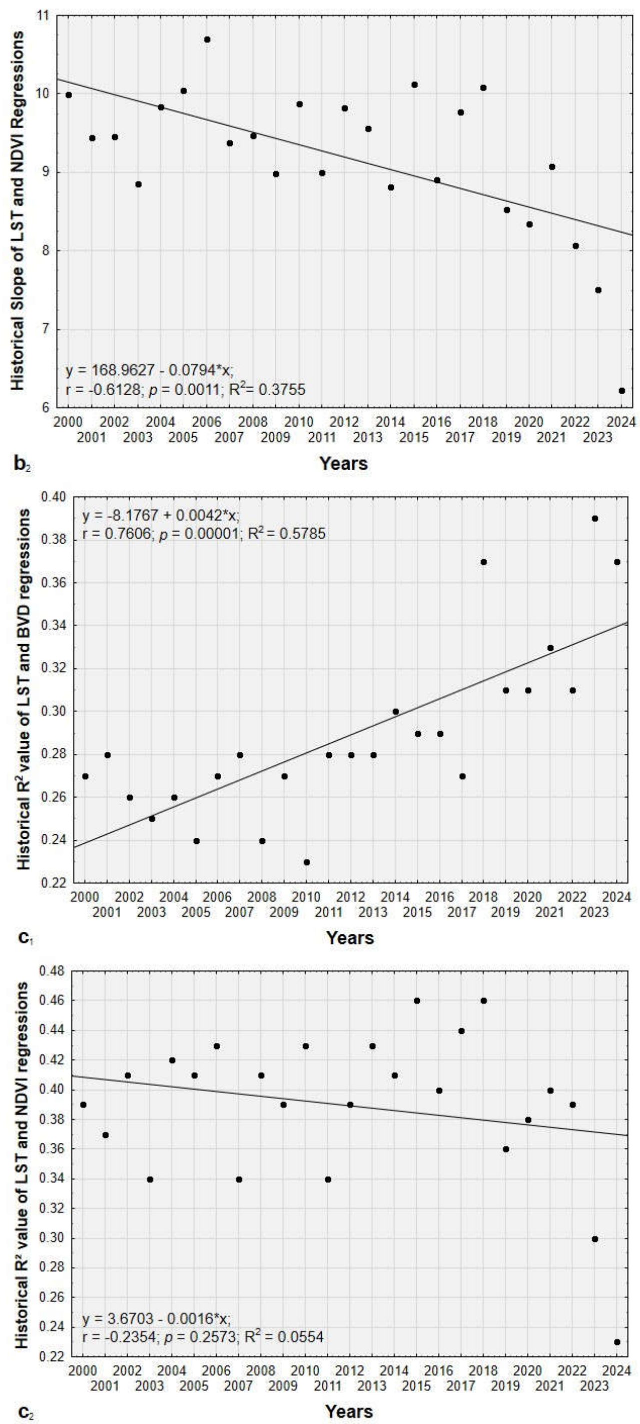

Figure 7. Linear regression performed between Building Volume Density (BVD) and LST (**a**1), vegetation density expressed by NDVI and LST (**a**2), and the historical trends in the regressions' slope (**b**1,**b**2) and coefficient of determination values (**c**1,**c**2). In **a** each point corresponds to a pixel of 1km².

4. Discussion

4.1. Data and Spatial Analysis of the UHI

The spatial and temporal pattern analyses of the Urban Heat Island (UHI) were performed using MOD11A2 V6.1. Each pixel in MOD11A2 represents the mean value derived from all corresponding MOD11A1 LST pixels recorded over the 8-day interval [25]. This approach reduces the effects of

Preprints.org (www.preprints.org) | NOT PEER-REVIEWED | Posted: 31 December 2024 doi:10.20944/preprints202412.2623.v1

punctual anomalies such as clouds or sensor errors by averaging data. It is therefore more reliable than products based on a single daily or instantaneous observation. In addition, MODIS LST data (including MOD11A2) have been extensively validated through comparisons with in situ measurements, which have consistently shown high accuracy under clear and stable atmospheric conditions [33,34]. With its 1km spatial resolution, MOD11A2 is also well suited for medium-scale studies such as urban-rural gradient analysis.

The spatial analysis of the urban heat island (UHI) was carried out within the urban-rural gradient of Kisangani city, using sampling areas randomly selected across various locations representing all cardinal and intercardinal directions within each zone of the gradient. Compared to an approach based on transects [30], or a method based on concentric zones [15], this approach not only enhances the data collected but also accounts for the substantial spatial variation that can arise perpendicular to a traditional transect. By incorporating variations over short distances, this method mitigates potential oversights that could be introduced by a concentric zone methodology [19].

4.2. Spatio-Temporal Patterns of Urban Heat Island (UHI)

In this study, we observed significant temporal variations in the spatial patterns of urban heat islands (UHI) between 2000 and 2024. During this period, the extent of medium UHI gradually expanded from 16 km² to 38 km², while high UHI increased from 9 km² to 19 km². Within the urban-rural gradient, significant annual variations in UHI are observed, with urban areas having significantly higher averages than peri-urban and rural areas. Several factors related to urban development, land use and land cover change (LULCC), and social and economic transformation, may explain these findings in the context of Kisangani city. Indeed, in general, rural landscapes are characterized by vegetation, while urban areas consist mainly of impervious surfaces such as concrete, pavements, rooftops, and compacted ground [18–35]. This land cover conversion in urban areas has a significant impact on the local microclimate and thermal environment, resulting in a relatively high heat absorption capacity and poor ventilation [35,36].

In the city of Kisangani, rapid population growth from 2000 to 2021 [37], has led to increasing urbanization, characterized by an expansion of urban and peri-urban areas and a significant reduction in natural areas [18,19]. This spatial transformation may have altered the thermal properties of the surface in the city of Kisangani, as artificial materials such as concrete and asphalt absorb and retain more solar radiation than natural surfaces. This phenomenon is one of the main factors behind the heat island effect [38–40]. Consequently, the expansion of these increasingly artificial areas would have contributed to the progression of medium and high UHI zones between 2000 and 2024 in Kisangani City, leading to significant variations of the UHI effect between the urbanization gradient zones. These results correspond to those observed in other cities. In Uganda, Li et al.[16], studied the urbanization trends and modifications in surface Urban Heat Islands (SUHI) within the Kampala urban cluster. Their analysis revealed that from 1995 to 2017, Kampala experienced substantial changes in its urban infrastructure. The urban land area grew from 12,133 hectares in 1995 to 25,389 hectares in 2016. Consequently, the extent of the Urban Heat Island increased significantly, rising from 22,910 hectares in 2003 to 27,900 hectares in 2016. This effect of urban expansion on microclimate was also observed in Accra, Ghana. In fact, Wemegah et al.[17], found the LST was significantly higher in urbanized and bare soil regions compared to areas with vegetation and water bodies.

Although land artificialization is less pronounced in peri-urban areas compared to urban zones, the findings of this study highlight its substantial influence on the urban heat island (UHI) effect relative to rural areas. Indeed, in peri-urban areas, the progressive conversion of natural landscapes into semi-artificial areas such as intensive agricultural fields, light infrastructure, or informal settlements, reduces the connectivity of vegetative cover, thereby weakening its ability to moderate local temperatures through processes like evaporation and transpiration, as well as by passively providing shade to surfaces that would otherwise absorb short-wave radiation [41]. Moreover, the surfaces created in peri-urban areas, although less dominated by concrete and asphalt than in urban

Preprints.org (www.preprints.org) | NOT PEER-REVIEWED | Posted: 31 December 2024 doi:10.20944/preprints202412.2623.v1

areas, are made of materials with higher thermal inertia than natural soils or surrounding vegetation. These absorb heat during the daytime and gradually release it at night, intensifying the thermal contrast between peri-urban and rural landscapes. Peri-urban areas are also influenced by the thermal effects of adjacent urban centers. The UHI effect generated within the city can extend to these peripheral areas through heat transfer driven by mixed convection, a phenomenon that is exacerbated by local atmospheric currents that transport warm air from the urban core to the surrounding peri-urban areas [42,43].

4.3. Impact of Building Architecture on the LST

This study has shown that the influence of building volume density (BVD) as a predictor of land surface temperature (LST) increases over time in the city of Kisangani, a trend evidenced by progressively higher slope and coefficients of determination values in the regression analyses. This increasing correlation suggests that as urban areas expand, with changes in urban architecture involving building geometry, particularly construction patterns with tall buildings situated closely together in small spaces, the capacity of these densely built environments to retain and emit heat intensifies.

This architectural model contributes to the phenomenon referred to as the "urban canyon"[5,6]. Indeed, since the end of the armed conflict between 1990 and 2000 [44], the city of Kisangani has experienced continuous spatial growth characterized by alternating processes of diffusion and coalescence [18]. This spatial growth is largely driven by economic operators, mainly from the east of the DRC, gradually exploiting interstitial spaces in Kisangani's urban center by constructing large commercial complexes and high-rise hotels. This progressive installation of these new buildings accentuates their spatial footprint and thus the canyon effect caused by increasing building density. This urban canyon effect influences various local conditions, including wind patterns, light availability, air quality, and temperature, thereby significantly exacerbating the intensification of urban heat islands [7]. In Kisangani, this could affect urban residents in various ways, shaping their comfort, air and water quality, access to ecological services, opportunities for recreation, and overall living conditions [9,10].

4.4. Effective and Resilient Mitigation Strategies of UHI

It should be noted that urbanization if properly managed, does not always lead to environmental degradation [16]. However, mitigating the UHI effect in Kisangani would require strategies tailored to its specific socio-economic, environmental, and climatic context. These effective and resilient solutions should integrate green infrastructure, urban planning, and community engagement. Indeed, the expansion of green spaces such as parks, urban forests, roadside vegetation, and green corridors connecting urban, peri-urban, and rural landscapes should lower surface and air temperatures through shading and evapotranspiration [41–45]. For Kisangani, leveraging its proximity to the Congo rainforest provides an opportunity to integrate indigenous plant species into urban landscapes. Previous studies have shown that in cities with a UHI effect, such as Hong Kong or Lisbon, the cooling effect of urban green spaces is more accentuated on hot and dry days [46,47]. In drier environments, rising temperatures and higher transpiration rates amplify the vegetation's humidifying effects [41–48]. Furthermore, protecting and restoring peri-urban vegetation can enhance temperature regulation while mitigating urban sprawl. In addition, encouraging the use of green roofs and vertical gardens can help reduce rooftop temperatures, provide insulation, and improve urban aesthetics. On the other hand, Malley et al. [14], highlighted that building design, including form, orientation, and layout, plays a crucial role in mitigating the urban heat island effect. Additionally, incorporating high-albedo (reflective) materials for structures and roadways can significantly decrease heat absorption.

Finally, to effectively address the impacts of urban heat islands (UHIs), it is imperative to strengthen land-use planning and management policies, particularly in urban and peri-urban areas. These policies should establish explicit guidelines to control urban sprawl and thus limit unplanned

 doi:10.20944/preprints202412.2623.v1

development in the city of Kisangani. To achieve this, it is essential to identify and prioritize critical areas for the conservation of green spaces and ecological corridors, thereby ensuring ecological connectivity and minimizing landscape artificialization. Furthermore, active engagement of local communities in land-use decision-making processes in peri-urban and rural regions is necessary to address socio-economic needs while also safeguarding environmental integrity. In addition, scientists should prioritize interdisciplinary approaches that integrate urban planning, climatology, ecology, and socio-economic studies. To maximize the impact of research, findings should be effectively communicated through scientific publications, policy briefs, and community engagement initiatives. Local communities should be made aware of the importance of green infrastructure and sustainable practices in reducing the UHI effect. Simplifying complex scientific concepts into accessible formats will encourage broader participation and support for mitigation efforts. Research institutions must ensure that their findings translate into actionable policies. This involves actively engaging with policymakers to integrate scientific evidence into urban planning and environmental conservation strategies. Furthermore, scenario analyses that simulate the long-term benefits of sustainable land-use practices can help demonstrate the value of these policies, fostering greater political will for implementation. To this end, capacity building is essential for sustaining research and mitigation efforts. Training programs should be designed to equip local researchers, urban planners, and practitioners while partnerships with international institutions can provide access to funding, expertise, and technological resources.

5. Conclusions

In this paper, a time series of MOD11A2 V6.1 data was used to map the spatial pattern of Urban Heat Islands (UHIs) in the fast-growing city of Kisangani between 2000 and 2024. Over the study period, the spatial pattern of UHI exhibits significant temporal variation. The areas with UHI values above 0°C have gradually expanded from 2000 to 2024, with significant annual UHI values, exceeding 0.1 and 0.2°C, consistently observed in the city center. Therefore, the spatial extent of medium UHI gradually expanded from 16 km² to 38 km², while high UHI increased from 9 km² to 19 km² between 2000 and 2024. Within the Urban-Rural Gradient, as expected, significant variations in both Land Surface Temperature (LST) and Urban Heat Island effect (UHI) are observed in 2024, with urban zones exhibiting substantially higher averages than peri-urban and rural zones. LST and UHI variations in peri-urban areas are also significantly different from rural areas. Furthermore, areas with maximum LST around 34°C and maximum UHI values of more than 0.2°C, are observed in urban zones, while peri-urban and rural zones reach maximum LST of 31°C and maximum UHI values of slightly more than 0.1°C. In addition, historical trends in annual land surface temperature (LST) and urban heat island (UHI) variations within each urbanization gradient zone from 2000 to 2024 are statistically significant ($p<0.05$). Similarly, between urbanization gradient zones, significant differences in the UHI annual variations are observed.

Regression analyses revealed that variations in Land Surface Temperature (LST) are significantly correlated with Building Volume Density (BVD) and vegetation density, expressed by the Normalized Difference Vegetation Index (NDVI). However, the influence of building volume density (BVD) as a predictor of land surface temperature (LST) increases over time in the city of Kisangani. This trend is evidenced by progressively higher slopes and coefficients of determination values. This increasing correlation suggests that as urban areas expand, with changes in urban architecture involving building geometry, particularly construction patterns with tall buildings situated closely together in small spaces, the capacity of these densely built environments to retain and emit heat intensifies. These findings highlight the importance of integrated development policies to effectively manage the interface that exists between urbanization, changes in landscape patterns, and the supply of ecosystem services. As urban and peri-urban areas expand, vegetation faces loss and fragmentation, weakening its ability to regulate the urban heat island (UHI) effect. However, the UHI mitigating strategies tailored to the specific socio-economic, environmental, and climatic context of Kisangani are increasingly essential. These effective and resilient solutions should integrate green

Preprints.org (www.preprints.org) | NOT PEER-REVIEWED | Posted: 31 December 2024 doi:10.20944/preprints202412.2623.v1

infrastructure, urban planning, and community engagement. Indeed, expanding green spaces, including parks, urban forests, roadside vegetation, and green corridors linking urban, peri-urban, and rural areas, should lower surface and air temperatures through shading and evapotranspiration. This holistic strategy offers a way to balance urban expansion and economic progress while preserving ecosystem services across the urban-rural gradient

Author Contributions: J.B.B., T.M.S., J.-P.P.M.T.H., K.R.S., Y.U.S., J.-F.B. and J.B. conceptualization, methodology, formal analysis. J.B.B. data collection and analysis. J.B.B. wrote the first draft of the article. J.B.B., T.M.S., P.T.W., J.E.M., J.M.T. and B.M.A. were responsible for proofreading the text. J.B.: validation and supervision. All authors have read and agreed to the published version of the manuscript.

Funding: This research was supported by the ERAIFT-AGRINATURA consortium, funded through the Development Cooperation Instrument (DCI) No. 41928 of the European Union. The authors express their gratitude to the European Union and the ERAIFT-AGRINATURA consortium for their financial support.

Data Availability Statement: Data can be made available by contacting the authors.

Conflicts of Interest: The authors declare no conflicts of interest.

References

1. Jato-espino, D. Spatiotemporal Statistical Analysis of the Urban Heat Island e Ff Ect in a Mediterranean Region. *Sustain. Cities Soc.*, **2019**, *46* (January), 101427. https://doi.org/10.1016/j.scs.2019.101427.
2. Dwivedi, A.; Khire, M. V. Application of Split- Window Algorithm to Study Urban Heat Island e Ff Ect in Mumbai through Land Surface Temperature Approach. *Sustain. Cities Soc.*, **2018**, *41* (October 2016), 865–877. https://doi.org/10.1016/j.scs.2018.02.030.
3. Kolokotroni, M.; Giannitsaris, I.; Watkins, R. The Effect of the London Urban Heat Island on Building Summer Cooling Demand and Night Ventilation Strategies. **2006**, *80*, 383–392. https://doi.org/10.1016/j.solener.2005.03.010.
4. Liu, K.; Su, H.; Zhang, L.; Yang, H.; Zhang, R.; Li, X. Analysis of the Urban Heat Island Effect in Shijiazhuang, China Using Satellite and Airborne Data. **2015**, 4804–4833. https://doi.org/10.3390/rs70404804.
5. Arnfield, A. J. Two Decades of Urban Climate Research : A Review of Turbulence , Exchanges of Energy and Water , and the Urban Heat Island. **2003**, *26*, 1–26. https://doi.org/10.1002/joc.859.
6. Oke, T. R. Boundary Layer Climates - 2nd Ed.; 2002.
7. Stewart, I. D.; Oke, T. R. Local Climate Zones for Urban Temperature Studies. *Am. Meteorol. Soc.*, **2012**. https://doi.org/10.1175/BAMS-D-11-00019.1.
8. Taha, H. Urban Climates and Heat Islands : Albedo , Evapotranspiration , and Anthropogenic Heat. **1997**, *25* (96), 99–103.
9. Candra, A.; Lecturer, K.; Nitivattananon, V. Factors Influencing Urban Heat Island in Surabaya , Indonesia. *Sustain. Cities Soc.*, **2016**, *27*, 99–105. https://doi.org/10.1016/j.scs.2016.07.006.
10. Prilandita, N. Perceptions and Responses to Warming in an Urban Environment: A Case Study of Bandung City, Indonesia. **2009**, *V* (1), 51–58.
11. Martínez, F.; Fernando, N.; Aragonés, N.; Benítez, P.; Buitrago, M. J.; Casas, I.; Cortés, M.; Dürr, U.; Herrera, D.; Izquierdo, A.; et al. Assessment of the Impact of the Summer 2003 Heat Wave on Mortality. **2004**, *18* (Supl 1), 250–258.
12. Garcia-Herrera, R.; Díaz, J.; Trigo, R. M.; Luterbacher, J.; Fischer, E. M. A Review of the European Summer Heat Wave of 2003 A Review of the European Summer Heat Wave of 2003. **2010**, *3389*. https://doi.org/10.1080/10643380802238137.
13. Zhang, H.; Qi, Z.; Ye, X.; Cai, Y.; Ma, W.; Chen, M. Analysis of Land Use / Land Cover Change , Population Shift , and Their Effects on Spatiotemporal Patterns of Urban Heat Islands in Metropolitan Shanghai , China. *Appl. Geogr.*, **2013**, *44*, 121–133. https://doi.org/10.1016/j.apgeog.2013.07.021.
14. Malley, C. O.; Piroozfarb, P. A. E.; Farr, E. R. P.; Gates, J. An Investigation into Minimizing Urban Heat Island (UHI) Effects : A UK Perspective. *Energy Procedia*, **2014**, *62* (0), 72–80. https://doi.org/10.1016/j.egypro.2014.12.368.
15. Mandal, J.; Pravin, P.; Samanta, S. Examining the Expansion of Urban Heat Island Effect in the Kolkata Metropolitan Area and Its Vicinity Using Multi-Temporal MODIS Satellite Data. *Adv. Sp. Res.*, **2022**, *69* (5), 1960–1977. https://doi.org/10.1016/j.asr.2021.11.040.
16. Li, X.; Stringer, L. C.; Chapman, S.; Id, M. D. How Urbanisation Alters the Intensity of the Urban Heat Island in a Tropical African City. **2021**, 1–18. https://doi.org/10.1371/journal.pone.0254371.
17. Wemegah, C. S.; Yamba, E. I.; Aryee, J. N. A.; Sam, F.; Amekudzi, L. K. Assessment of Urban Heat Island Warming in the Greater Accra Region. *Sci. African*, **2020**, *8*, e00426. https://doi.org/10.1016/j.sciaf.2020.e00426.

18. Balandi, J. B.; Meniko, J.-P. P. T. H.; Sambieni, K. R.; Sikuzani, Y. U.; Bastin, J.-F.; Musavandalo, C. M.; Elangi Langi, J. M.; Selemani, T. M.; Mweru, J. M.; Bogaert, J. Urban Sprawl and Changes in Landscape Patterns : The Case of Kisangani City and Its Periphery (DR Congo). **2023**, 1–14. https://doi.org/10.3390/land12112066.
19. Balandi, J. B.; Meniko, J.-P. P. T. H.; Sambieni, K. R.; Sikuzani, Y. U.; Bastin, J.-F.; Musavandalo, C. M.; Nguba, T. B.; Jesuka, R.; Sodalo, C.; Pika, L. M.; Bogaert, J. Anthropogenic Effects on Green Infrastructure Spatial Patterns in Kisangani City and Its Urban – Rural Gradient. **2024**. https://doi.org/10.3390/land13111794.
20. UN-Habitat. Habitat III RD Congo: Rapport Final. **2015**, 1–93.
21. Sabongo, P. Y. Etude Comparative de La Structure et de La Diversité Des Forêts à Gilbertiodendron Dewevrei (De Wild) J.Léonard Des Régions de Kisangani et de l'Ituri (RD Congo), Thèse de Doctorat. Université de Kisangani, 2015.
22. Kottek, M.; Grieser, J.; Beck, C.; Rudolf, B.; Rubel, F. World Map of the Köppen-Geiger Climate Classification Updated. *Meteorol. Zeitschrift*, **2006**, *15* (3), 259–263. https://doi.org/10.1127/0941-2948/2006/0130.
23. Gabriel, K. B.; Omer, N. T. Etude Socio-Économique Des Conflits Des Guerres Armées Dans La Ville de Kisangani et Sa Périphérie En Province de La Tshopo (1997 à 2006). *IJRDO - J. Soc. Sci. Humanit. Res.*, **2022**, No. 5, 318–324.
24. European Commission. GHSL Data Package 2023, Publications Office of the European Union, Luxembourg; 2023. https://doi.org/10.2760/098587.
25. Wan, Z. MODIS Land Surface Temperature Products Users ' Guide. **2013**.
26. Azizi, S.; Azizi, T. Urban Climate Dynamics: Analyzing the Impact of Green Cover and Air Pollution on Land Surface Temperature—A Comparative Study Across Chicago, San Francisco, and Phoenix, USA. **2024**.
27. Didan, K.; Munoz, A. B.; Huete, A. MODIS Vegetation Index User ' s Guide (MOD13 Series). **2015**, *2015* (June).
28. Rendana, M.; Mohd, W.; Idris, R.; Rahim, S. A.; Abdo, H. G.; Almohamad, H.; Abdullah, A.; Dughairi, A.; Al-mutiry, M. Relationships between Land Use Types and Urban Heat Island Intensity in Hulu Langat District , Selangor , Malaysia. *Ecol. Process.*, **2023**, No. July. https://doi.org/10.1186/s13717-023-00446-9.
29. Huang, Q.; Huang, J.; Yang, X.; Fang, C.; Liang, Y. Quantifying the Seasonal Contribution of Coupling Urban Land Use Types on Urban Heat Island Using Land Contribution Index : A Case Study in Wuhan ,. *Sustain. Cities Soc.*, **2019**, *44* (October 2018), 666–675. https://doi.org/10.1016/j.scs.2018.10.016.
30. Marando, F.; Salvatori, E.; Sebastiani, A.; Fusaro, L.; Manes, F. Regulating Ecosystem Services and Green Infrastructure : Assessment of Urban Heat Island Effect Mitigation in the Municipality of Rome , Italy. *Ecol. Modell.*, **2019**, *392* (July 2018), 92–102. https://doi.org/10.1016/j.ecolmodel.2018.11.011.
31. Sambieni, K. R. Dynamique Du Paysage de La Ville Province de Kinshasa Sous La Pression de La Périurbanisation: L'infrastructure Verte Comme Moteur d'aménagement. Thèse de Doctorat, Université de Liège, et ERAIFT. **2019**, 1–261.
32. Angel, S.; Parent, J.; Civco, D. L.; Blei, A.; Potere, D. The Dimensions of Global Urban Expansion: Estimates and Projections for All Countries, 2000-2050. *Prog. Plann.*, **2011**, *75* (2), 53–107. https://doi.org/10.1016/j.progress.2011.04.001.
33. Lu, L.; Zhang, T.; Wang, T. Evaluation of Collection-6 MODIS Land Surface Temperature Product Using Multi-Year Ground Measurements in an Arid Area of Northwest China. **2018**, *1*. https://doi.org/10.3390/rs10111852.
34. Wan, Z.; Zhang, Y.; Zhang, Q.; Li, Z. Validation of the Land-Surface Temperature Products Retrieved from Terra Moderate Resolution Imaging Spectroradiometer Data. **2002**, *83*, 163–180.
35. Wen, C.; Mamtimin, A.; Feng, J.; Wang, Y.; Yang, F.; Huo, W.; Zhou, C.; Li, R.; Song, M.; Gao, J.; et al. Diurnal Variation in Urban Heat Island Intensity in Birmingham : The Relationship between Nocturnal Surface And. **2023**.
36. Dutta, D.; Rahman, A.; Paul, S. K.; Kundu, A. Urban Climate Impervious Surface Growth and Its Inter-Relationship with Vegetation Cover and Land Surface Temperature in Peri-Urban Areas of Delhi. *Urban Clim.*, **2021**, *37* (January), 100799. https://doi.org/10.1016/j.uclim.2021.100799.
37. INS. Population de La Ville de Kisangani Repartie En Sexe, de 1990 à 2021. Kisangani 2022.
38. Haodong, L.; Zheng, H.; Wu, L.; Deng, Y.; Chen, J.; Zhang, J. Spatiotemporal Evolution in the Thermal Environment and Impact Analysis of Drivers in the Beijing – Tianjin – Hebei Urban Agglomeration of China from 2000 to 2020. **2024**.
39. Ren, J.; Shi, K.; Kong, X.; Zhou, H. On-Site Measurement and Numerical Simulation Study on Characteristic of Urban Heat Island in a Multi-Block Region in Beijing , China. *Sustain. Cities Soc.*, **2023**, *95* (April), 104615. https://doi.org/10.1016/j.scs.2023.104615.
40. Lima, I.; Scalco, V.; Lamberts, R. Energy & Buildings Estimating the Impact of Urban Densification on High-Rise Office Building Cooling Loads in a Hot and Humid Climate. *Energy Build.*, **2019**, *182*, 30–44. https://doi.org/10.1016/j.enbuild.2018.10.019.

 doi:10.20944/preprints202412.2623.v1

41. Yan, M.; Chen, L.; Leng, S.; Sun, R. Effects of Local Background Climate on Urban Vegetation Cooling and Humidification : Variations and Thresholds. *Urban For. Urban Green.*, **2023**, *80* (December 2022), 127840. https://doi.org/10.1016/j.ufug.2023.127840.
42. Ziyan; Paschalis, A.; Mijic, A.; Meili, N.; Manoli, G.; Reeuwijk, M. Van; Fatichi, S. Urban Climate A Mechanistic Assessment of Urban Heat Island Intensities and Drivers across Climates. *Urban Clim.*, **2022**, *44*, 101215. https://doi.org/10.1016/j.uclim.2022.101215.
43. Omidvar, H.; Bou-zeid, E.; Li, Q.; Mellado, J. Plume or Bubble ? Mixed-Convection Flow Regimes and City-Scale Circulations. **2020**. https://doi.org/10.1017/jfm.2020.360.
44. Koluwa, S. K. De La Reparation Des Victimes de La Guerre de Six Jours à Kisangani. *J. Soc. Sci. Humaniyies Res.*, **2020**, *5* (11), 44–56.
45. Fengjiao, C.; Feng, S.; Feng, Q.; Yujie, W.; Tailong, Z.; Haiying, Y. Research Advances in the Influence of Vegetation on Urban Heat Island Effect. **2020**, *56*.
46. Kwan, P.; Fung, C. K. W.; Jim, C. Y. Seasonal and Meteorological Effects on the Cooling Magnitude of Trees in Subtropical Climate. *Build. Environ.*, **2020**, *177* (April), 106911. https://doi.org/10.1016/j.buildenv.2020.106911.
47. Oliveira, S.; Andrade, H.; Vaz, T. The Cooling Effect of Green Spaces as a Contribution to the Mitigation of Urban Heat : A Case Study in Lisbon. *Build. Environ.*, **2011**, *46* (11), 2186–2194. https://doi.org/10.1016/j.buildenv.2011.04.034.
48. Cheung, P. K.; Jim, C. Y.; Siu, C. T. Effects of Urban Park Design Features on Summer Air Temperature and Humidity in Compact-City Milieu. *Appl. Geogr.*, **2021**, *129* (February), 102439. https://doi.org/10.1016/j.apgeog.2021.102439.